Table S1. The salt bridges at the p110α-p85 α interface in PI3Kα.

p85α		p110α		PI3Kα	PI3Kα△nSH2
Domain	Residue	Domain	Residue		
nSH2	R348	C2	D454	99.9%	0%
nSH2	K374	C2	D369	40.1%	0%
nSH2	K379	Helical	E542	99.3%	0%
nSH2	K379	Helical	E545	74.8%	0%
nSH2	K382	Helical	E547	30.2%	0%
nSH2	K419	Helical	E579	63.4%	0%
nSH2	D421	Helical	K548	41.8%	0%
nSH2	D421	Helical	K573	89.0%	0%
nSH2	R340	Kinase	D1029	100%	0%
nSH2	E341	Kinase	R1023	99.9%	0%
nSH2	E345	Kinase	K1024	99.1%	0%
nSH2	R348	Kinase	D1017	100%	0%
nSH2	D359	Kinase	K1030	65.9%	0%
nSH2	K363	Kinase	E1037	52.5%	0%
iSH2	E489	ABD	R79	96.2%	99.8%
iSH2	E496	ABD	K100	72.2%	74.1%
iSH2	R534	ABD	E23	100%	99.4%
iSH2	R557	C2	E469	56.1%	82.3%
iSH2	D569	C2	R412	56.1%	30.3%
iSH2	R574	C2	E453	99.1%	0%
iSH2	K575	C2	E418	60.0%	84.1%
iSH2	D464	Kinase	K944	88.6%	0%

The salt bridge interacting residue pairs are considered when the distance between any of atoms in the acidic and basic residues is within the cut-off distance of 3.5 Å. The salt bridges with the probability > 30% are shown. The residue contact with significant change upon nSH2 release is highlighted in blue.

Table S2. The hydrophobic interactions at the p110α-p85 α interface in PI3Kα.

p85α		p110α		PI3Kα	PI3Kα△nSH2
Domain	Residue	Domain	Residue		
iSH2	M479	ABD	W11	100%	100%
iSH2	A483	ABD	W11	100%	100%
iSH2	A483	ABD	F95	100%	100%
iSH2	A486	ABD	W11	97.1%	99.2%
iSH2	A486	ABD	V73	100%	100%
iSH2	A486	ABD	A77	96.7%	95.1%
iSH2	A486	ABD	F95	100%	100%
iSH2	A486	ABD	F98	89.6%	97.8%
iSH2	F487	ABD	W11	98.2%	95.3%
iSH2	F487	ABD	V73	100%	100%
iSH2	F487	ABD	F95	100%	100%
iSH2	I493	ABD	L25	100%	100%
iSH2	I493	ABD	V71	100%	100%
iSH2	I493	ABD	V73	100%	100%
iSH2	I493	ABD	P98	100%	100%
iSH2	F494	ABD	L25	100%	100%
iSH2	F494	ABD	I31	100%	99.9%
iSH2	F494	ABD	F98	100%	100%
iSH2	I524	ABD	M30	100%	99.9%
iSH2	I524	ABD	P57	100%	100%
iSH2	I524	ABD	L58	100%	99.9%
iSH2	L531	ABD	L25	100%	100%
iSH2	L531	ABD	M30	100%	99.8%
iSH2	L531	ABD	I31	100%	100%
iSH2	I538	ABD	F95	98.8%	98.7%
iSH2	I538	ABD	F98	97.7%	97.4%
iSH2	P568	C2	I351	99.4%	99.6%
iSH2	P568	C2	A415	77.7%	38.0%
iSH2	P568	C2	P421	90.1%	99.2%
iSH2	P568	C2	L422	84.9%	100%
iSH2	I571	C2	A415	70.9%	15.9%
iSH2	I571	C2	P421	97.7%	99.2%
iSH2	I571	C2	L452	97.4%	100%

The hydrophobic interacting residue pairs are considered when the distance between any of atoms in the hydrophobic residues is within the cut-off distance of 6.5 Å. The hydrophobic interactions with the probability > 30% are shown. The residue contact with significant change upon nSH2 release is highlighted in blue.

Figure S1. The time-dependent domain (*a*) angel and (*b*) distance profiles of p110α upon nSH2 release.

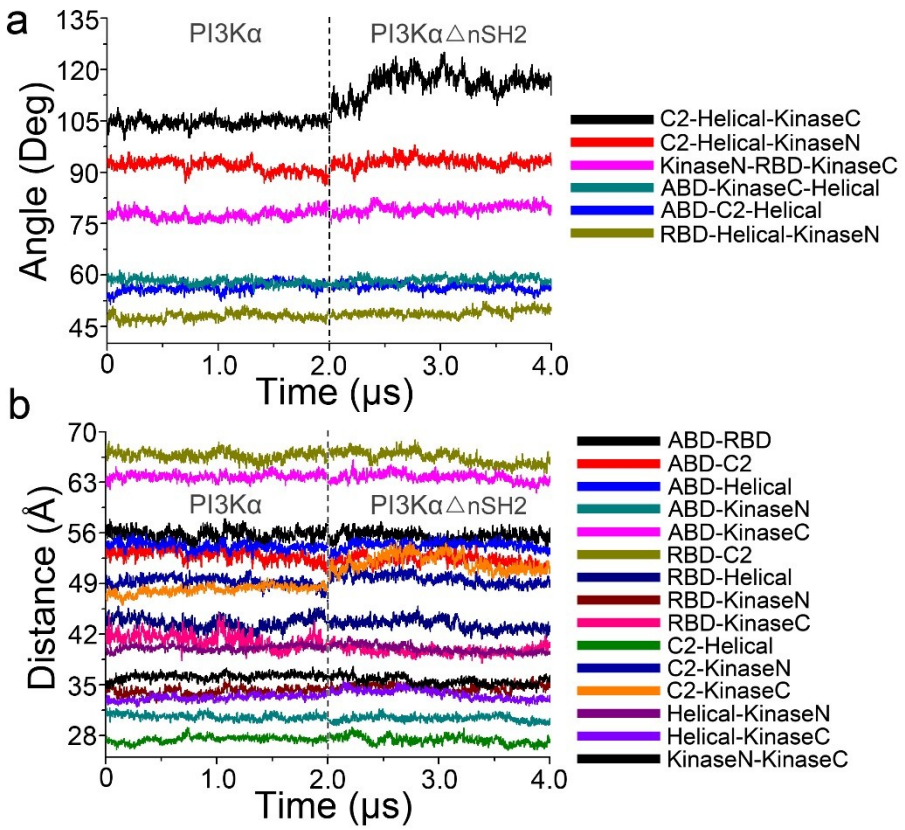

Figure S2. Results of principal component analysis (PCA). MD snapshots for inactive PI3Kα and active PI3KαΔnSH2 are projected onto the first and second PCs.

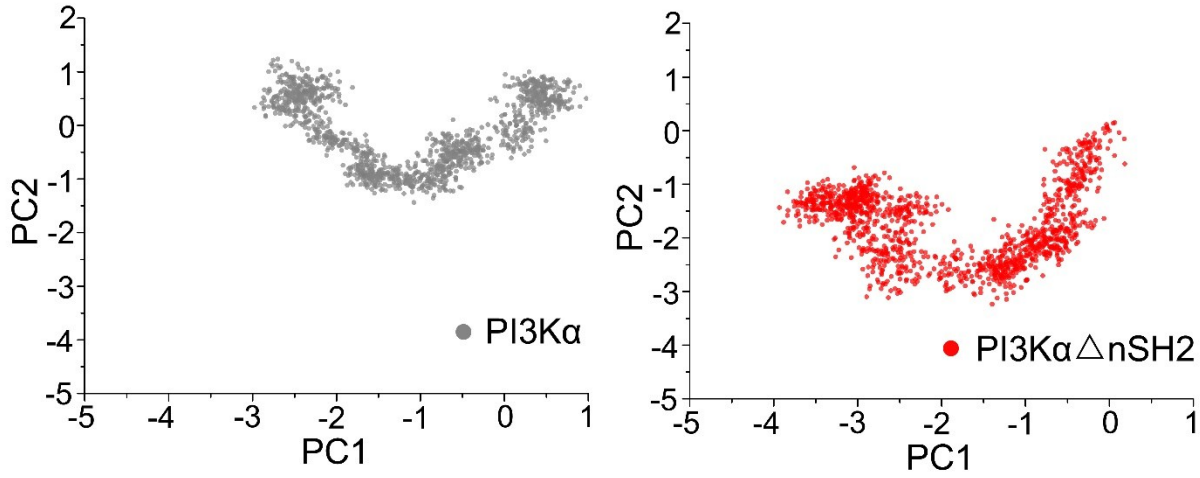

Figure S3. Disruption of the salt bridges at (*a*) iSH2-C2 interface and (*b*) iSH2-kinase interface, and (*c*) the change of the solvent-accessible surface areas (SASA) of kinaseC upon PI3Kα activation by nSH2 release.

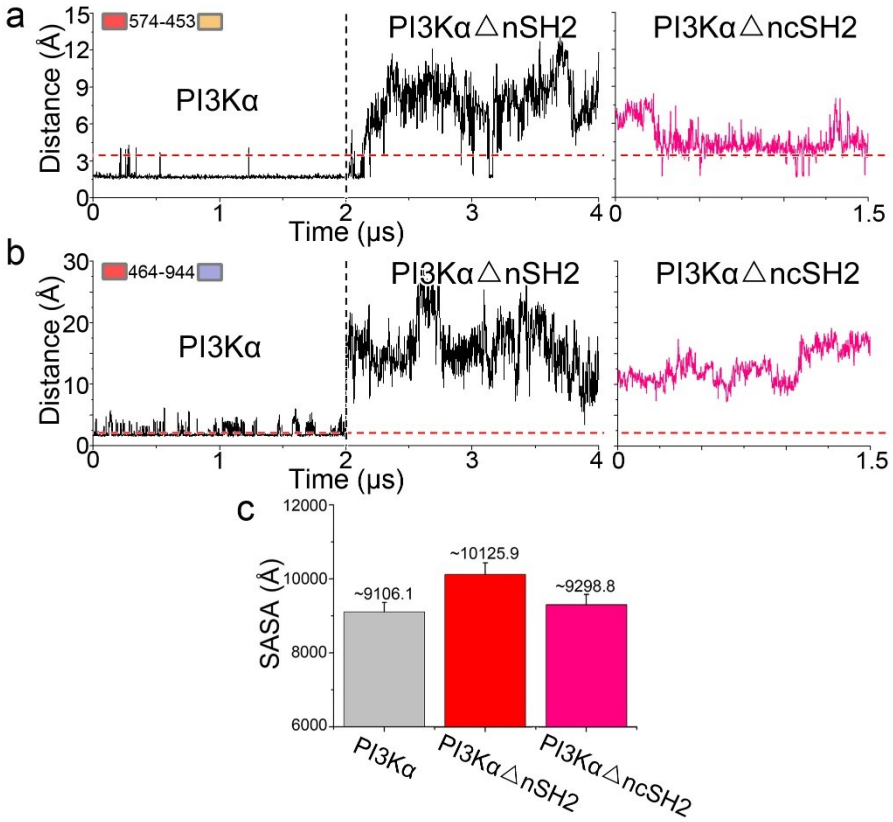

Figure S4. Conformation change of ABD-RBD linker in PI3Kα upon nSH2 release.

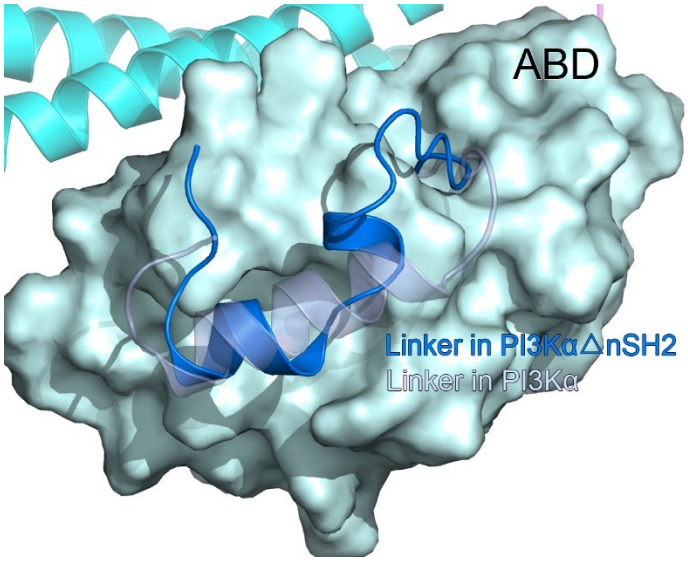

Figure S5. (*a*) Membrane contacting probability and (*b*) the snapshot for residues in iSH2 domain interacting with membrane in the active PI3Kα with nSH2 released. The membrane surface is defined by the positions of $_{kinase}Glu^{726}$, $_{kinase}His^{1047}$ and $_{kinase}Lys^{942}$ in the kinase domain. The residues with high membrane contacting probability is highlighted in orange.

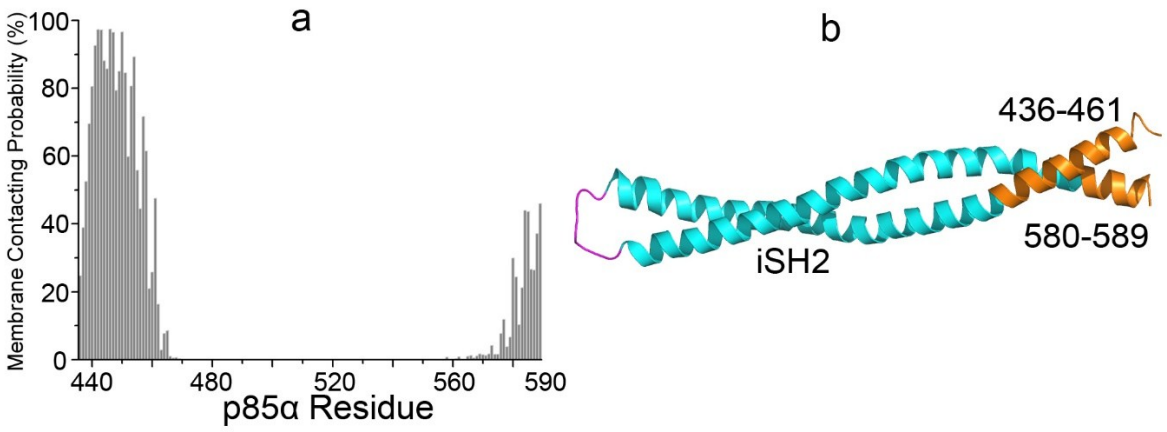

Figure S6. 2D RMSD plots for ABD, RBD, C2, helical domain, kinaseN in p110α upon PI3Kα activation by nSH2 release.

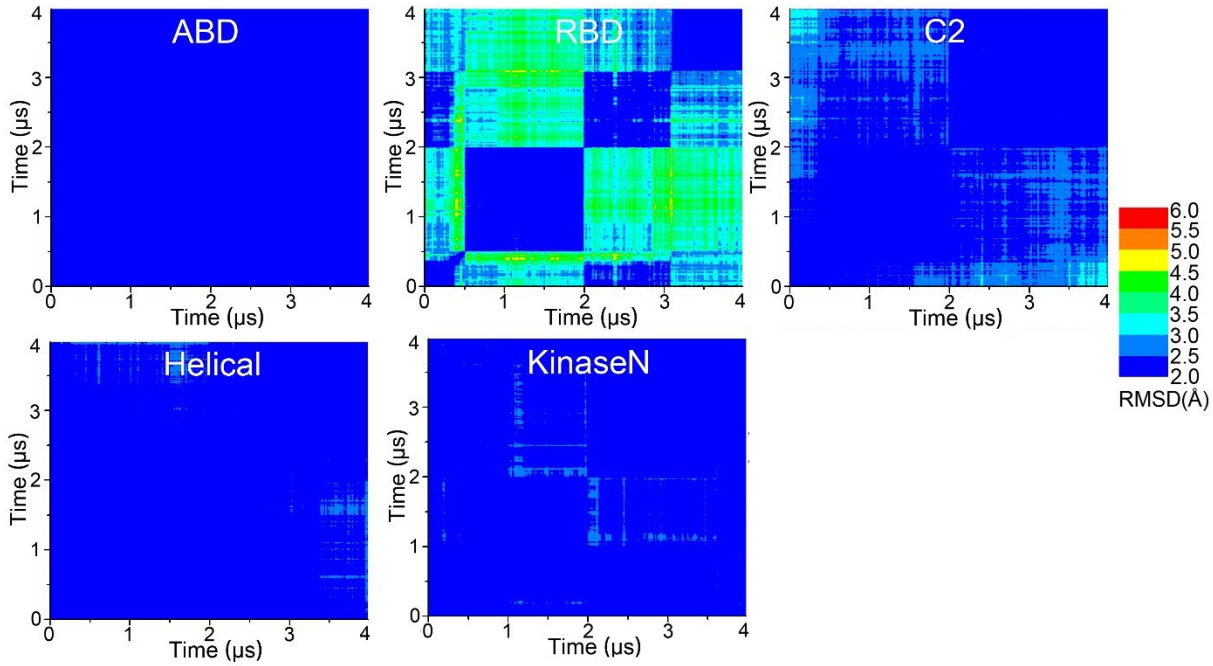

Figure S7. Structural rearrangement of kinaseC in PI3Kα upon nSH2 release. (*a*) The residue-based RMSD values show that six fragments in kinaseC experience significant conformational change. (*b*) The snapshot shows that these fragments (highlighted in orange) are located at the surface of kinaseC.

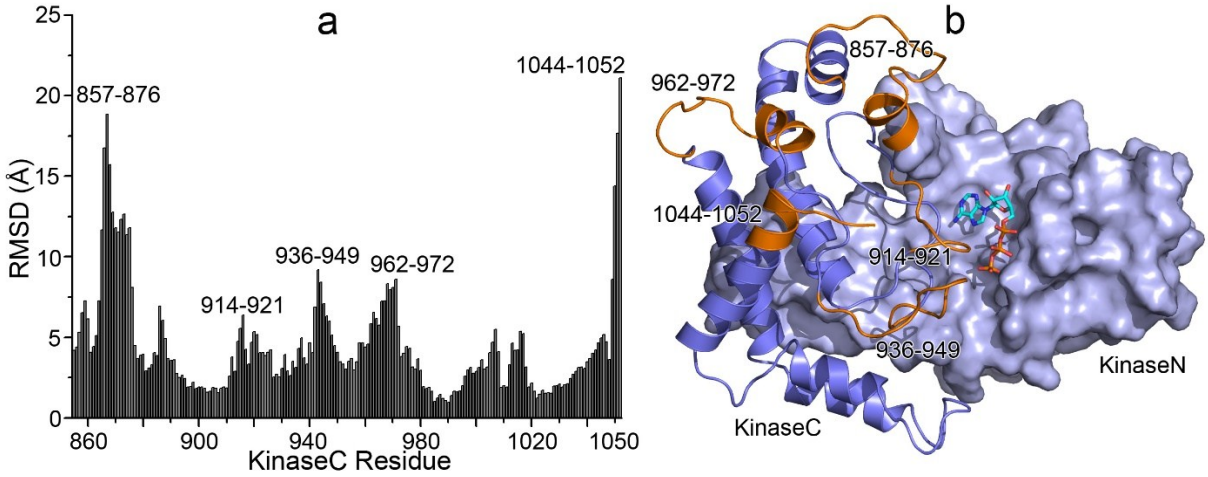

Figure S8. Catalytic site in the active PI3Kα. (a) Schematic illustration of catalytic site of PI3Kα. The distances of (b) $Lys^{941-944}$ and (c) His^{936} to ATP are reduced upon nSH2 release.

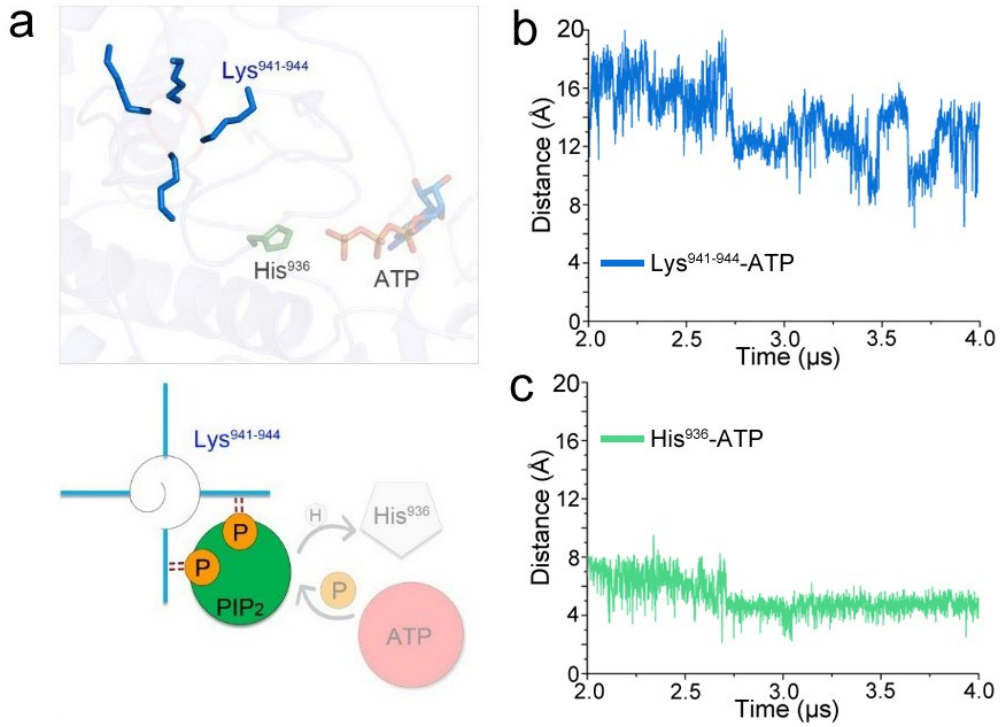

Figure S9. cSH2 domain in PI3Kα. By two different strategies, cSH2 is modeled into PI3Kα (*a*) based on the crystal structure of PI3Kβ, and (*b*) by docking. In both PI3Kα structures, cSH2 interacts with kinase domain in p110α. The RMSF profiles for the (*c*) superimposed and (*d*) docked cSH2 in PI3Kα suggest that the interactions of cSH2 to p110α are less stable, compared to nSH2 and iSH2 in p85α.

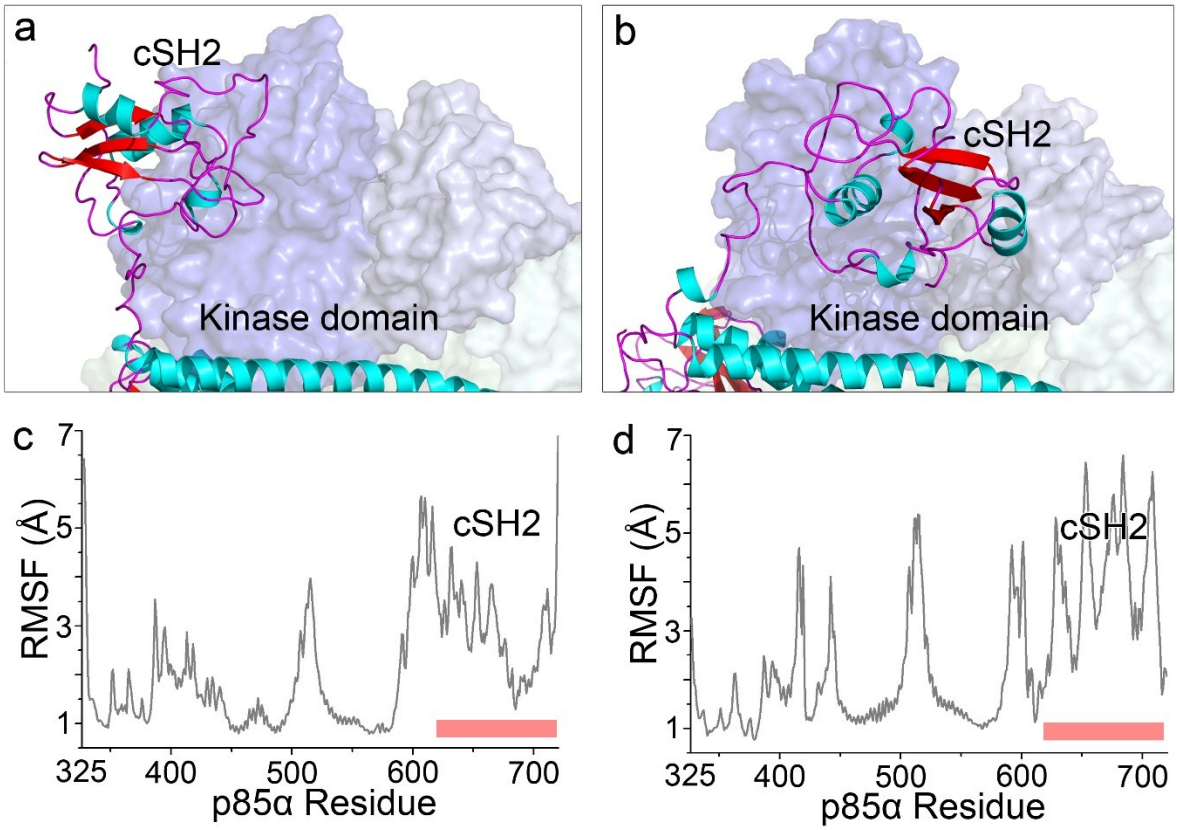

Figure S10. Schematic illustration for PI3Kα activation by nSH2 release. In the inactive PI3Kα, the kinase domain cannot access the membrane because of because of steric clash of iSH2 domain, and the PIP_2-ATP distance is too far for substrate phosphorylation. The pY motifs in RTK activate PI3Kα by releasing the nSH2 domain. nSH2 release triggers significant conformation change in p110α, making kinaseC more exposed for interacting with the membrane. Upon the nSH2 release, the structural arrangement in kinaseC lead to a reduced PIP_2-ATP distance suitable for substrate phosphorylation. Ras interacts with the RBD in p110α recruits PI3Kα onto membrane.

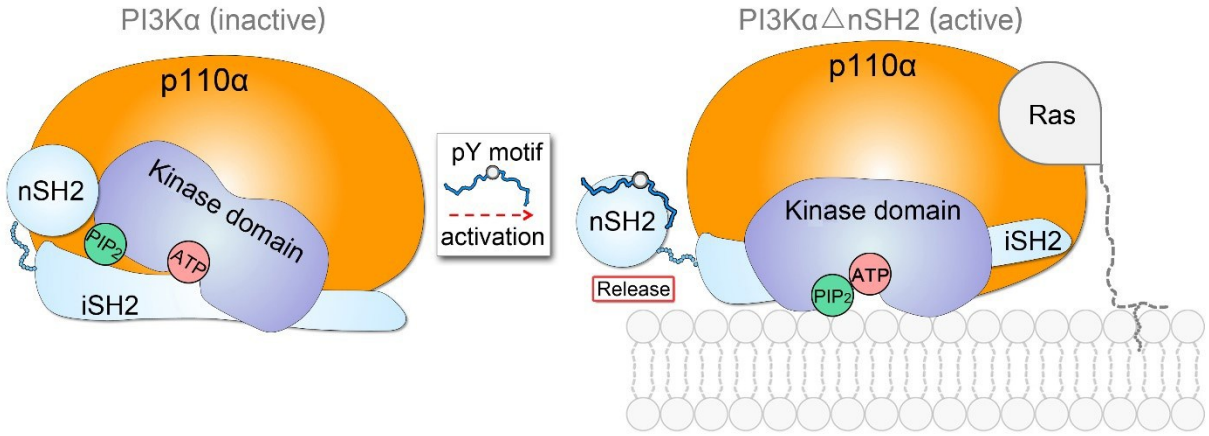

Figure S11. Summary of simulation systems.